

Paper:

Study on Combining Two Faster R-CNN Models for Landslide Detection with a Classification Decision Tree to Improve the Detection Performance

Asadang Tanatipuknon^{*1,*2,†}, Pakinee Aimmanee^{*1}, Yoshihiro Watanabe^{*3},
Ken T. Murata^{*4}, Akihiko Wakai^{*5}, Go Sato^{*6}, Hoang Viet Hung^{*7},
Kanokvate Tungpimolrut^{*2}, Suthum Keeratvittayanun^{*2}, and Jessada Karnjana^{*2}

^{*1}Sirindhorn International Institute of Technology, Thammasat University
Pathum Thani, Thailand

[†]Corresponding author, E-mail: m6222040484@g.siiit.tu.ac.th

^{*2}National Electronics and Computer Technology Center (NECTEC),
National Science and Technology Development Agency, Pathum Thani, Thailand

^{*3}School of Engineering, Tokyo Institute of Technology, Tokyo, Japan

^{*4}National Institute of Information and Communications Technology (NICT), Tokyo, Japan

^{*5}Graduate School of Science and Technology, Gunma University, Gumma, Japan

^{*6}Graduate School of Environmental Informations, Teikyo Heisei University, Tokyo, Japan

^{*7}Faculty of Civil Engineering, Thuyloi University, Hanoi, Vietnam

[Received November 30, 2020; accepted April 4, 2021]

This study aims to improve the accuracy of landslide detection in satellite images by combining two object detection models based on a faster region-based convolutional neural network (Faster R-CNN) with a classification decision tree. The proposed method combines the predicted results from the two Faster R-CNN models and classifies their features with a classification decision tree to generate a bounding-box that surrounds the landslide area in the input image. The first Faster R-CNN model is trained by using a training set of color images (RGB images). The second model is trained by using grayscale images that represent digital elevation models (DEMs). The results from both models are used to construct features for training a classification decision tree. The resulting bounding-box is selected from the following four classes: the box obtained from the RGB model, the box obtained from the DEM model, the intersection of those two boxes, and the smallest box that contains the union of them. The evaluation results show that the proposed method is better than the RGB model in terms of accuracy, precision, recall, F-measure, and Intersection-over-Union (IoU) score. It is slightly better than the DEM model in almost all evaluation metrics, except the precision.

Keywords: Faster R-CNN, classification decision tree, landslide detection, satellite imagery

1. Introduction

A landslide is a dangerous natural disaster that occurs in extensive areas, especially mountainous regions. According to a report of the World Health Organization (WHO), from 1998 to 2017, landslides caused almost 20,000 deaths and affected about five million people worldwide [1]. Therefore, preventing damage, and monitoring and identifying landslide-prone areas are crucial in risk assessment, reduction, and management. The monitoring system can be done locally, such as deploying a sensor network [2], or remotely, such as analyzing satellite images [3] or using an unmanned aerial vehicle (UAV) attached with digital cameras [4].

Recently, machine learning and neural-network-based approaches have been applied for landslide detection [3, 5–7]. The results obtained from these research findings are promising.

A state-of-the-art method in this area has shown that combining pieces of information from a satellite image and the digital elevation model (DEM) to train a convolutional neural network (CNN) can significantly improve the overall performance [8]. Inspired by that work, we have hypothesized that instead of combining information at the input-data level, combining the results of two models at the output level may improve the overall performance. Thus, this paper tests this to experimentally show that the idea of combining two models can improve the accuracy over that obtained by a sole model.

To the best of our knowledge, our combination of two models for monitoring landslides has not been reported in the literature. In this work, we implement two Faster region-based CNNs (Faster R-CNNs) that take different



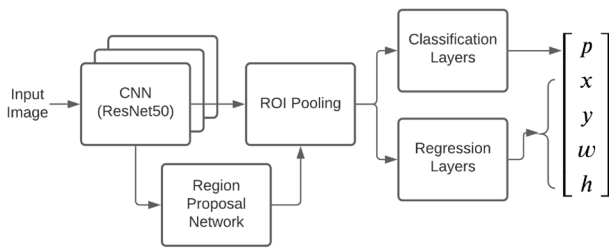


Fig. 1. Structure of a Faster R-CNN.

input-image types and detect landslide areas in images. Then, a simple classification tree is developed to combine the results from the two models.

The rest of this paper is organized as follows. Section 2 describes the background knowledge used for the proposed method, the Faster R-CNN and the classification decision tree. Section 3 provides the details of the proposed framework. The experiments, results, and evaluations are given in Section 4. The discussion is in Section 5, and Section 6 concludes this work.

2. Background

This section provides a short review of the Faster R-CNN and the classification decision tree, which are the basis of our proposed method.

2.1. Faster Region-Based Convolutional Neural Network (R-CNN)

A state-of-the-art object detection network based on a convolutional neural network is the Faster R-CNN [9]. It is an improvement of the conventional fast R-CNN [10], which detects objects and shows the results by drawing rectangular boxes around the detected objects. The Faster R-CNN is improved from the fast R-CNN by replacing the part that generates regions of interest with a region proposal network (RPN).

The architecture of the Faster R-CNN is illustrated in Fig. 1. The Faster R-CNN first generates a feature map by convoluting the input image. The convolutional neural network used in this project is a pre-trained ResNet-50 [11], which is trained from the ImageNet database [12]. The RPN uses boxes, called anchor boxes, to slide on the whole image, generating the object proposals. Then, the Faster R-CNN resizes the feature maps to a dimension that matches the input dimension of fully connected layers. Finally, the fully connected layers classify the objects and regress to box \mathbf{b} , which is the output, as shown in Fig. 1. Box \mathbf{b} is composed of five elements: p , x , y , w , and h , as depicted in Fig. 2. The first element p is a confidence score that represents the probability of the object inside this box. x and y are the coordinates of the left-corner point, and w and h are the width and the height of the box, respectively.

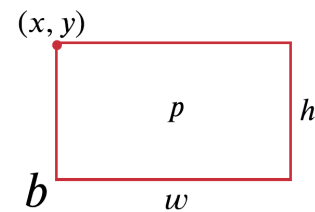


Fig. 2. Results of the Faster R-CNN, bounding box \mathbf{b} with five elements.

2.2. Classification Decision Tree

The classification decision tree is a predictive model where the target variable is discrete [13]. This study uses the classification tree because of its advantages concerning the tree construction cost and the classifying speed of new data. Also, for simple data sets, its accuracy is acceptable [14]. In terms of the tree structure, leaves are class labels, and branches are feature conjunctions that lead to the leaves. Thus, the classification tree is a collection of rules that map a set of explanatory variables (or an attribute set) to a response variable (or a class). These rules are formulated by a process called *recursive partitioning* [13].

Let D_t denote the set of training records (i.e., the attribute set and a class) that are associated with node t . Let y denote a set of class labels, i.e., $y = \{y_1, y_2, \dots, y_c\}$. The two basic steps applied for growing a decision are as follows [15].

1. If all records in D_t are in the same class y_t , then t is a leaf labeled as y_t .
2. If records in D_t belong to more than two classes, the records are partitioned into two smaller subsets by applying an attribute test condition. Thus, two children of t are created. Each subset of D_t is associated with each child depending upon the outcome of the test condition. Then, both steps are recursively repeated and applied to each child.

3. Proposed Framework

The proposed framework consists of three parts, which are the two Faster R-CNN models, feature vector construction, and a classification tree model, as illustrated in Fig. 3. In Fig. 3, the RGB image and the DEM image are the inputs. The first Faster R-CNN model is trained to detect a landslide in an RGB satellite image. Thus, it takes an RGB satellite image as the input. It outputs a rectangular box that bounds a landslide area. Similarly, the second Faster R-CNN model is trained to detect a landslide in a grayscale image representing a digital elevation model (DEM) at the same location as the RGB satellite image that was fed to the first Faster R-CNN. Thus, it takes a DEM image as the input and produces another rectangular box as the output. Both Faster R-CNNs share the same structure, as shown in Fig. 1.

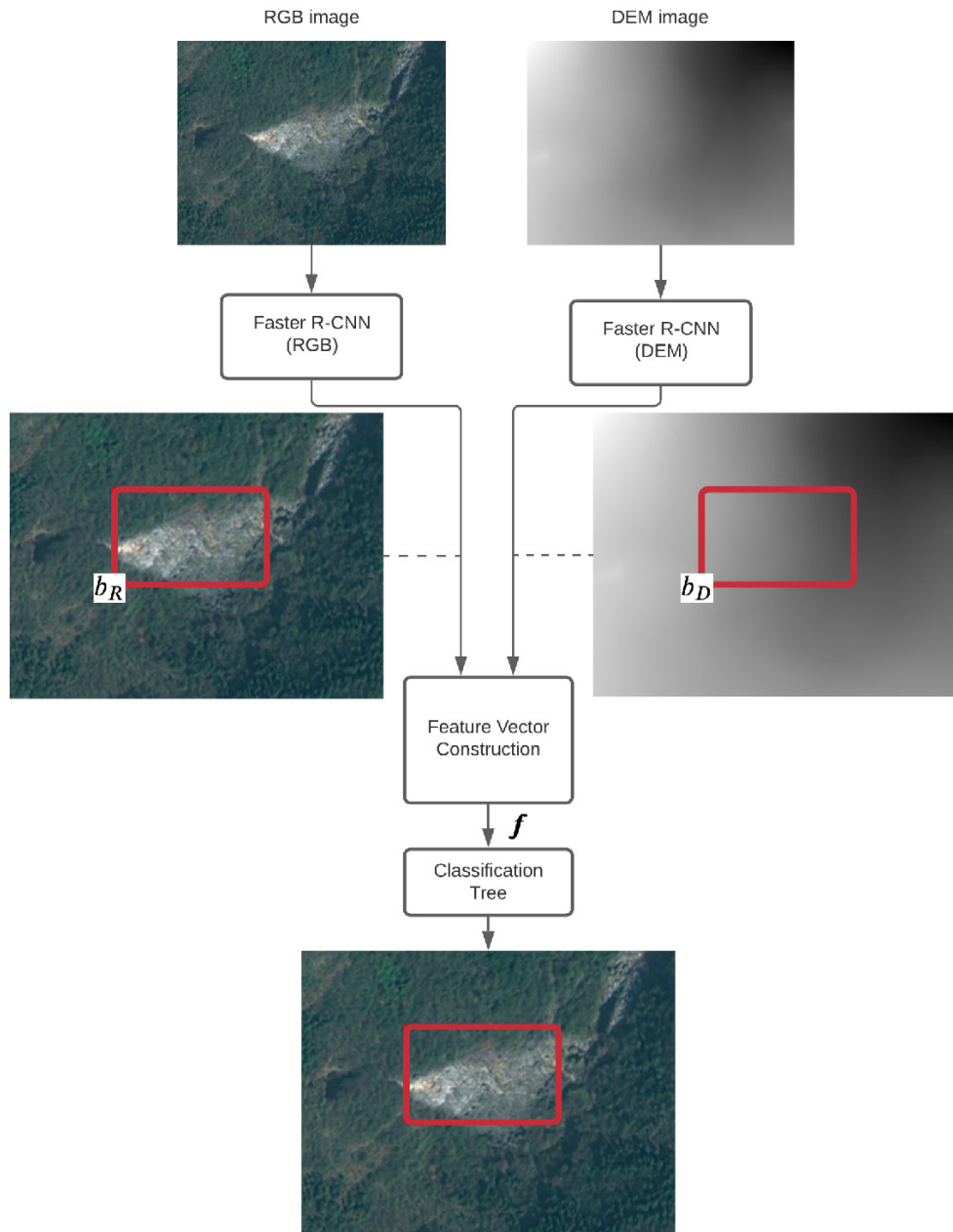


Fig. 3. Proposed framework.

The output boxes from the first part are input into the feature vector construction that generates a feature vector of four components. Let the RGB and DEM output boxes be denoted by $\mathbf{b}_R = [p_R \ x_R \ y_R \ w_R \ h_R]^T$ and $\mathbf{b}_D = [p_D \ x_D \ y_D \ w_D \ h_D]^T$, respectively. Let $\text{IoU}(\alpha, \beta)$ denote the results of performing the Intersection-over-Union (IoU) operator on α and β [6], which are formulated as

$$\text{IoU}(\alpha, \beta) = \frac{|\alpha \cap \beta|}{|\alpha \cup \beta|}, \dots \dots \dots (1)$$

where $|\alpha \cap \beta|$ is the intersection of boxes \mathbf{b}_α and \mathbf{b}_β . Similarly $|\alpha \cup \beta|$ is the union of the two boxes, as shown

in Fig. 4.

The feature vector \mathbf{f} is constructed by

$$\mathbf{f} = \begin{bmatrix} \text{IoU}(\mathbf{b}_R, \mathbf{b}_D) \\ \text{IoU}(\mathbf{b}_R \cap \mathbf{b}_D, \mathbf{b}^*) \\ p_R \\ p_D \end{bmatrix}, \dots \dots \dots (2)$$

where \mathbf{b}^* is the smallest box that contains $\mathbf{b}_R \cup \mathbf{b}_D$.

Finally, the decision tree based on the four components in \mathbf{f} selects one of the following four boxes as the output: \mathbf{b}_R , \mathbf{b}_D , $\mathbf{b}_R \cap \mathbf{b}_D$, and \mathbf{b}^* .

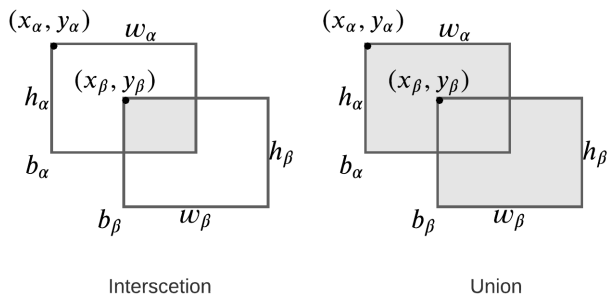


Fig. 4. Intersection-over-Union illustration.

4. Experiment and Evaluation

The dataset used in our experiments was taken from an open-access dataset provided by Ji et al. [8]. It has 770 RGB TripleSat-satellite images that contain landslide areas. The study site is in Bijie city, which is located in the northwest of Guizhou province, China. It covers an area of approximately 27,000 m² [8]. Guizhou province is located in the plateau region of southwest China, and it has extensive carbonate rock distribution and karst development. This province suffers from various kinds of geological disasters, such as debris flows, landslides, and ground cracks due to large crustal uplift and deformation [8].

All images in the dataset were captured from May to August, 2018. The dataset also provides grayscale images that represent the digital elevation models (DEM) of those RGB images. The ground-truth images are also included in the dataset. The sizes of the satellite images vary, depending on landslide regions in the images. The RGB image resolution is 0.8 m, and the accuracy of the DEM elevation is 2 m.

In our experiments, we randomly divided the dataset into two sets: a training set and a testing set. The training set consists of 700 images, and the testing set comprises 70 images. The RGB images in the training set were used to train the Faster R-CNN to detect landslide areas in the RGB images. Similarly, the DEM images were used to train another Faster R-CNN to detect landslide areas in the DEM images. The structure of the Faster R-CNN is illustrated in Fig. 1. The dimensions of the input of ResNet-50 are 32 × 32 × 3. The anchor sizes are 16 × 16, 16 × 32, and 32 × 16. The optimizer is the stochastic gradient descent with momentum. The initial learning rate is set to 0.001. The minibatch size is set to 1. The number of epochs is set to 7.

To train the classification tree, we first calculate a class score γ , defined by the following equation:

$$\gamma = \max\{\text{IoU}(\mathbf{b}_R, \mathbf{b}_G), \text{IoU}(\mathbf{b}_D, \mathbf{b}_G), \text{IoU}(\mathbf{b}^*, \mathbf{b}_G), \text{IoU}(\mathbf{b}_R \cap \mathbf{b}_D, \mathbf{b}_G)\}, \dots \quad (3)$$

where \mathbf{b}_G is the ground-truth box.

Targets (classes) used in the tree training process were assigned by the following criteria. If $\gamma = \text{IoU}(\mathbf{b}_R, \mathbf{b}_G)$, the tree classifies the feature vector \mathbf{f} as of the \mathbf{b}_R class, and the resulting box is \mathbf{b}_R . If $\gamma = \text{IoU}(\mathbf{b}_D, \mathbf{b}_G)$, the tree

classifies \mathbf{f} as of the \mathbf{b}_D class, and the resulting box is \mathbf{b}_D . If $\gamma = \text{IoU}(\mathbf{b}^*, \mathbf{b}_G)$, the tree classifies \mathbf{f} as of the \mathbf{b}^* class, and the resulting box is \mathbf{b}^* . If $\gamma = \text{IoU}(\mathbf{b}_R \cap \mathbf{b}_D, \mathbf{b}_G)$, the tree classifies \mathbf{f} as of the $\mathbf{b}_R \cap \mathbf{b}_D$ class, and the resulting box is $\mathbf{b}_R \cap \mathbf{b}_D$.

Five measures are used to evaluate the proposed method: accuracy, precision, recall, F-measure, and IoU [16–19]. Let N be the total number of pixels of the input image. Let TP, TN, FP, and FN be the numbers of true-positive pixels, true-negative pixels, false-positive pixels, and false-negative pixels, respectively. The accuracy is the ratio correctness of prediction from both positive and negative classes.

$$\text{Accuracy} = \frac{\text{TP} + \text{TN}}{N} \dots \dots \dots \quad (4)$$

The precision is the completeness of an answer with respect to a positive class domain.

$$\text{Precision} = \frac{\text{TP}}{\text{TP} + \text{FP}} \dots \dots \dots \quad (5)$$

The recall is the completeness of getting all correct answers.

$$\text{Recall} = \frac{\text{TP}}{\text{TP} + \text{FN}} \dots \dots \dots \quad (6)$$

The following equation formulates the F-measure:

$$\text{F-measure} = 2 \times \frac{\text{precision} \times \text{recall}}{\text{precision} + \text{recall}} \dots \dots \quad (7)$$

The accuracy, correctness, and completeness measures range from 0 to 1; the higher the value, the better the performance.

We use the F-measure instead of other measurements such as success rate (SR) and modified SR (MSR) [20] because of the following reasons. First, according to the definition of SR, SR is the ratio between the number of successfully predicted landslides and the total number of actual landslides. In other words,

$$\text{SR} = \frac{\text{TP}}{\text{TP} + \text{FN}} \dots \dots \dots \quad (8)$$

Thus, SR is the recall. It can be seen that SR does not take false positives into consideration. MSR is a modified version of SR that considers false positives. It is defined as

$$\text{MSR} = \frac{1}{2} \left(\frac{\text{TP}}{\text{TP} + \text{FN}} \right) + \frac{1}{2} \left(\frac{\text{TN}}{\text{FP} + \text{TN}} \right) \dots \quad (9)$$

It should be noted that MSR weights true positives and true negatives equally. In our opinion, MSR is not suitable for landslide detection in satellite images where most landslide areas are small in comparison with the input satellite images. The reason is that TN in such a case is high even though the algorithm does not correctly detect a landslide area. Therefore, the F-measure, which also considers false positives but ignores true negatives, is more suitable than MSR in this sense. We chose the F-measure because it is a measure that tells the overall performance of the completeness of getting the ground-truth solutions

Table 1. Performance comparison between the proposed method and the Faster R-CNN models.

	R-CNN (RGB)	R-CNN (DEM)	Proposed method
Accuracy	0.97	0.97	0.97
Precision	0.85	0.87	0.86
Recall	0.64	0.75	0.77
F-measure	0.71	0.78	0.79
IoU	0.61	0.66	0.67

and accuracy of the results.

In this study, we compared the proposed method to the Faster R-CNN models that were trained to solely detect landslide areas from RGB or DEM images. The experimental results are shown in **Table 1**.

It can be seen that the proposed method is better than the Faster R-CNN model for the RGB satellite images in all measures. It is also slightly better than the Faster R-CNN model for the DEM images in almost all measures, except the precision. Therefore, the results of this study support the idea that combining information from two neural networks with the classification tree can result in overall performance improvement. Examples of the results of each model are shown in **Fig. 5**, and **Fig. 6** compares the results.

5. Discussion

The proposed method shows that combining the two Faster R-CNN models can enhance landslide detection performance compared to using only one model. The evaluation results show that the proposed method outperforms the model for RGB images. It is slightly better than the model for DEM images in all measures except the precision. It should be noted that, in practice, DEM images alone cannot be used to analyze landslide detection.

As demonstrated in this study, the improvement from combining the two models might not be of general significance since the combination model we used in this study is a simple decision tree with only four features. We will study the methods of combination models such as a Dempster-Shafer theory [21] for our future work. Besides the combination model, the object detection accuracy and the training dataset also affect the proposed method. The region-based object detection can locate the object only in the bounding box. Currently, there are other techniques to detect an object, such as pixel-based object detection. Moreover, pixel-based classification methods are available for object detection [22, 23], which we will use in our future research.

Another issue to be discussed in this section is a performance comparison between the proposed method and the Faster R-CNN [9], of which its input is a combination of satellite image and DEM image. This comparison aims to examine the results from two cases: output-level combination and input-level combination. The per-

formance comparison is shown in **Table 2**. It can be seen that both output-level-combination case and input-level-combination case are comparable. However, the proposed method (i.e., a model with output-level combination) has two advantages over the Faster R-CNN with the input-level combination. First, the model with the output-level combination is more flexible than the model with the input-level combination. The reason is that the latter always requires the DEM image as a part of its input. In contrast, the former does not, i.e., the DEM image is not mandatory. Second, the model with output-level combination has room for improvement as a combination model, as mentioned earlier in the previous paragraph.

6. Conclusion

This paper reported the performance improvement of landslide detection in satellite images, based on convolutional neural networks with a classification decision tree. The contribution of this paper is that we experimentally show that combining two Faster R-CNN models with a simple decision tree can result in better evaluation scores than those obtained by the Faster R-CNN model alone.

We trained two Faster R-CNNs to detect landslide areas. The first model's input is the RGB satellite image. The second model's input is the grayscale DEM image. A feature vector is then constructed from the outputs of both models before it is fed to a decision tree. The decision tree is trained using features in the feature vector to select or combine the output boxes from both models. The experimental results showed that the proposed method is better than the Faster R-CNN model for RGB satellite images in all measures. Furthermore, it is also slightly better than the Faster R-CNN model for the DEM images in almost all measures, except the precision.

Acknowledgements

This study is supported by the Thailand Advanced Institute of Science and Technology (TAIST), National Science and Technology Development Agency (NSTDA), and Tokyo Institute of Technology under the TAIST-Tokyo Tech program. Also, this work has been partially supported by the ASEAN Committee on Science, Technology and Innovation (COSTI) under the ASEAN Plan of Action on Science, Technology and Innovation (APASTI) funding scheme and by e-ASIA JRP funding scheme.

References:

- [1] World Health Organization (WHO), "Landslides," <https://www.who.int/health-topics/landslides> [accessed September 11, 2020]
- [2] E. Intrieri, G. Gigli, F. Mugnai, R. Fanti, and N. Casagli, "Design and implementation of a landslide early warning system," *Engineering Geology*, Vol.147-148, pp. 124-136, 2012.
- [3] S. N. K. B. Amit and Y. Aoki, "Disaster detection from aerial imagery with convolutional neural network," *Proc. of 2017 Int. Electronics Symp. on Knowledge Creation and Intelligent Computing (IES-KCIC)*, pp. 239-245, 2017.
- [4] U. Niethammer, M. James, S. Rothmund, J. Travalletti, and M. Joswig, "UAV-based remote sensing of the Super-Sauze landslide: Evaluation and results," *Engineering Geology*, Vol.128, pp. 2-11, 2012.
- [5] O. Ghorbanzadeh, T. Blaschke, K. Gholamnia, S. R. Meena,

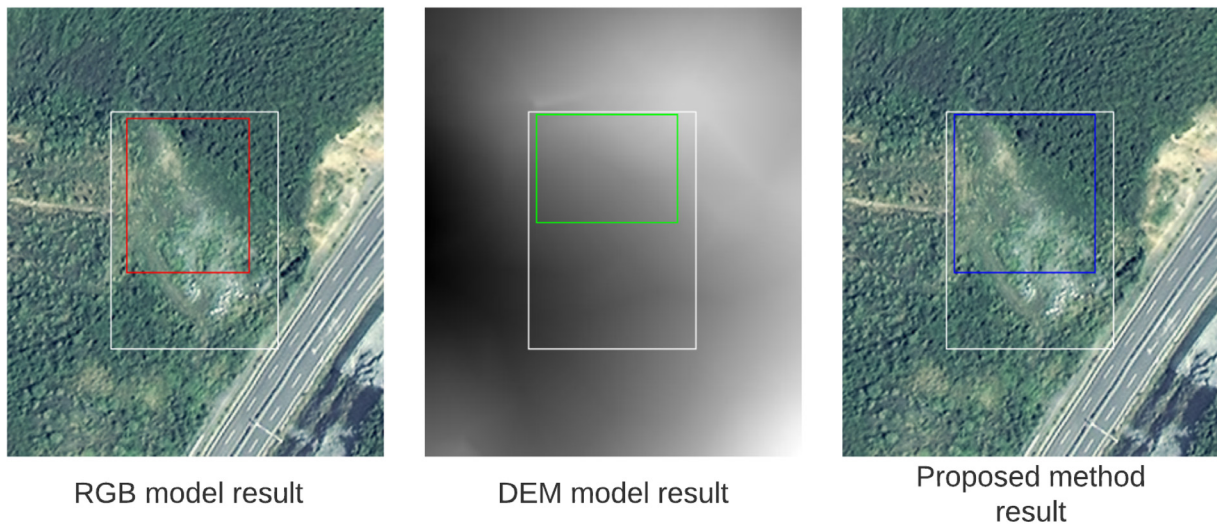


Fig. 5. Examples of the results of the RGB model (red), DEM model (green), and the proposed method (blue) in comparison with the ground truth (white).



Fig. 6. Examples of result comparison in three satellite images, the red box, green box, blue box, and white box, are the results of the RGB model, DEM model, the proposed method, and ground truth, respectively. Remark to the middle picture, the red box is the same as the proposed method box, so it doesn't show.

Table 2. Performance evaluation between the proposed method and Faster R-CNN model [9].

	Accuracy	Precision	Recall	F-measure	IoU
Faster R-CNN [9], of which its input is the combination of satellite images and DEM image	0.98	0.82	0.78	0.76	0.65
Proposed method	0.97	0.97	0.77	0.79	0.67

- D. Tiede, and J. Aryal, "Evaluation of different machine learning methods and deep-learning convolutional neural networks for landslide detection," *Remote Sensing*, Vol.11, No.2, Article No.196, 2019.
- [6] H. Rezaatofghi, N. Tsoi, J. Gwak, A. Sadeghian, I. Reid, and S. Savarese, "Generalized intersection over union: A metric and a loss for bounding box regression," *Proc. of 2019 IEEE/CVF Conf. on Computer Vision and Pattern Recognition*, pp. 658-666, 2019.
- [7] R. Soeters and C. J. Van Westen, "Slope instability recognition, analysis, and zonation," A. K. Turner and R. L. Schuster (Eds.), "Landslides: Investigation and mitigation (Transportation Research Board Special Report 247)," pp. 129-177, National Academy of Science, 1996.
- [8] S. Ji, D. Yu, C. Shen, W. Li, and Q. Xu, "Landslide detection from an open satellite imagery and digital elevation model dataset using attention boosted convolutional neural networks," *Landslides*, Vol.17, No.6, pp. 1337-1352, 2020.
- [9] S. Ren, K. He, R. Girshick, and J. Sun, "Faster R-CNN: Towards real-time object detection with region proposal networks," *Proc. of the 28th Int. Conf. on Neural Information Processing Systems (NIPS'15)*, Vol.1, pp. 91-99, 2015.
- [10] R. Girshick, "Fast R-CNN," *Proc. of 2015 IEEE Int. Conf. on Computer Vision (ICCV)*, pp. 1440-1448, 2015.
- [11] K. He, X. Zhang, S. Ren, and J. Sun, "Deep residual learning for image recognition," *Proc. of 2016 IEEE Conf. on Computer Vision and Pattern Recognition (CVPR)*, pp. 770-778, 2016.

- [12] Stanford Vision Lab, Stanford University, and Princeton University, "ImageNet," <https://image-net.org> [accessed February 1, 2021]
- [13] L. Breiman, J. Friedman, C. J. Stone, and R. A. Olshen, "Classification and regression trees," CRC Press, 1984.
- [14] M. Pal and P. M. Mather, "An assessment of the effectiveness of decision tree methods for land cover classification," *Remote Sensing of Environment*, Vol.86, No.4, pp. 554-565, 2003.
- [15] P.-N. Tan, M. Steinbach, and V. Kumar, "Introduction to data mining," 1st Edition, Pearson Education, 2016.
- [16] M. Buckland and F. Gey, "The relationship between Recall and Precision," *J. of the American Society for Information Science*, Vol.45, No.1, pp. 12-19, 1994.
- [17] M. Story and R. G. Congalton, "Accuracy assessment: A user's perspective," *Photogrammetric Engineering and Remote Sensing*, Vol.52, No.3, pp. 397-399, 1986.
- [18] P. Lu, Y. Qin, Z. Li, A. C. Mondini, and N. Casagli, "Landslide mapping from multi-sensor data through improved change detection-based Markov random field," *Remote Sensing of Environment*, Vol.231, Article No.111235, 2019.
- [19] S. Nowozin, "Optimal decisions from probabilistic models: The intersection-over-union case," *Proc. of 2014 IEEE Conf. on Computer Vision and Pattern Recognition (CVPR)*, pp. 548-555, 2014.
- [20] J. C. Huang and S. J. Kao, "Optimal estimator for assessing landslide model performance," *Hydrology and Earth System Sciences*, Vol.10, No.6, pp. 957-965, 2006.
- [21] K. Sentz and S. Ferson, "Combination of evidence in Dempster-Shafer theory," Sandia National Laboratories, doi: 10.2172/800792, 2002.
- [22] S. Mohajerani and P. Saeedi, "Cloud-Net: An end-to-end cloud detection algorithm for Landsat 8 imagery," *Proc. of 2019 IEEE Int. Geoscience and Remote Sensing Symp. (IGARSS 2019)*, pp. 1029-1032, 2019.
- [23] S. L. Phung, A. Bouzerdoum, and D. Chai, "Skin segmentation using color pixel classification: Analysis and comparison," *IEEE Trans. on Pattern Analysis and Machine Intelligence*, Vol.27, No.1, pp. 148-154, 2005.



Name:
Asadang Tanatipuknon

Affiliation:
Master's Degree Student under TAIST-Tokyo Tech program, Sirindhorn International Institute of Technology (SIIT), Thammasat University

Address:
Phahonyothin Road, Khlong Nueng, Khlong Luang District, Pathum Thani 12120, Thailand

Selected Publications:

- "Unsupervised Change Detection in Multi-temporal Satellite Images Based on Structural Patch Decomposition and k -means Clustering for Landslide Monitoring," *Proc. of the 8th Int. Symp. on Integrated Uncertainty in Knowledge Modelling and Decision Making (IUKM 2020)*, pp. 259-269, 2020.
 - "Improving Accuracy of Dissolved Oxygen Measurement in an Automatic Aerator-Control System for Shrimp Farming by Kalman Filtering," *Proc. of the Computational Intelligence in Information Systems Conf. (CIIS 2018)*, pp. 145-156, 2018.
-

Name:
Pakinee Aimmanee

Affiliation:
Sirindhorn International Institute of Technology (SIIT), Thammasat University
Address:
131 Moo 5 Tivanont Road, Bangkadi, Meung, Patum Thani 12000, Thailand

Name:
Yoshihiro Watanabe

Affiliation:
Tokyo Institute of Technology
Address:
4259-G2-31 Nagatsuta, Midori-ku, Yokohama, Kanagawa 226-8503, Japan

Name:
Ken T. Murata

Affiliation:
National Institute of Information and Communications Technology (NICT)
Address:
4-2-1 Nukui-Kitamachi, Koganei, Tokyo 184-8795, Japan

Name:
Akihiko Wakai

Affiliation:
Professor, Gunma University
Address:
1-5-1 Tenjincho, Kiryu, Gunma 376-8515, Japan

Name:

Go Sato

Affiliation:

Professor, Graduate School of Environmental Informations, Teikyo Heisei
University

Address:

4-21-2 Nakano, Nakano-ku, Tokyo 164-8530, Japan

Name:

Hoang Viet Hung

Affiliation:

Associate Professor of Geotechnical Engineering, Thuyloi University

Address:

175 Tay Son Street, Dong Da District, Hanoi, Vietnam

Name:

Kanokvate Tungpimolrut

Affiliation:

Researcher, Advanced Control and Electronics Research Group, National
Electronics and Computer Technology Center (NECTEC)

Address:

112 Thailand Science Park, Khlong Luang, Pathum Thani 12120, Thailand

Name:

Suthum Keerativittayanun

Affiliation:

National Electronics and Computer Technology Center (NECTEC)

Address:

112 Thailand Science Park, Khlong Luang, Pathum Thani 12120, Thailand

Name:

Jessada Karnjana

Affiliation:

Researcher, National Electronics and Computer Technology Center
(NECTEC)

Address:

112 Thailand Science Park, Khlong Luang, Pathum Thani 12120, Thailand
